CHAPTER - II

PREPARATION OF FERRITES AND X-RAY DIFFRACTION STUDIES

CHAPTER-II

PREPARATION OF FERRITES AND X-RAY DIFFRACTION STUDIES

2.1 INTRODUCTION :

Simple, mixed and sdubstitutional ferrites can be prepared by various methods[1,2,3]. Ferrites are industrially important materials as they possess suitable electrical and magnetic properties. The ferrites are generally prepared by two methods - (1) chemical method and (2) standard ceramic technique. Due to some limitations of chemical method, mostly the standard ceramic technique is used[4,5,6]. The technique is economic and involves mechanism of solid state reaction.

2.2 MECHANISM OF SOLID STATE REACTION :

Mechanism is discussed on the basis of diffusion of components involving divalent metal oxide MO and Fe_2O_3. In initial configuration there is only one phase boundary between reactants. After nucleation of ferrite, the boundary is replaced by two phase boundaries, one between MO and MFe_2O_4 and other, ferrite and Fe_2O_3.

In this state further progress of reaction can only take place by transport of reactants through ferrite phase. The transfer mechanism takes place in three ways which lead to the ferrite formation. According to Wagner[7,8] only cation migrate in opposite directions, the oxygen ions are essentially stationary. In second mode of transfer mechanism, diffusion of cation is compensated by an associated flux of anions instead of another cation migration. The third mode of transfer mechanism involves diffusion of iron through ferrite layer in the reduced state Fe^{2+}.[8]

2.3 THE GENERAL FORMULA OF SYSTEM :

The general formula of our ferrite system is $Zn_xCu_{1-x}Fe_2O_4$ doped with the rare earth Nb^{+5}, 0.02 and 0.05 mole at. % where x = 0, 0.2, 0.4, 0.6, 0.8 and 1.0.

2.4 RAW MATERIALS :

AR grade Fe_2O_3, ZnO and CuO supplied by Koch Light Laboratories Ltd., Colnbrook Berks, England and Thomas Baker and Company, London and Nb metal from Rare Earth, India were used for the preparation.

2.5 WEIGHING :

The various oxides were weighed on single pan micro balance of least count 10^{-4} gms and were mixed according to their molecular weight percentage.

MILLING :

The oxides mixed in the molecular weight proportions were taken in agate morter and were mechanically blended in AR grade acetone for two hours so as to form the intimate mixture. The mixtures were dried and were carefully transferred to clean and dry platinum crucibles.

2.6 FLOWCHART OF THE STAGES IN THE FERRITE PREPARATION :

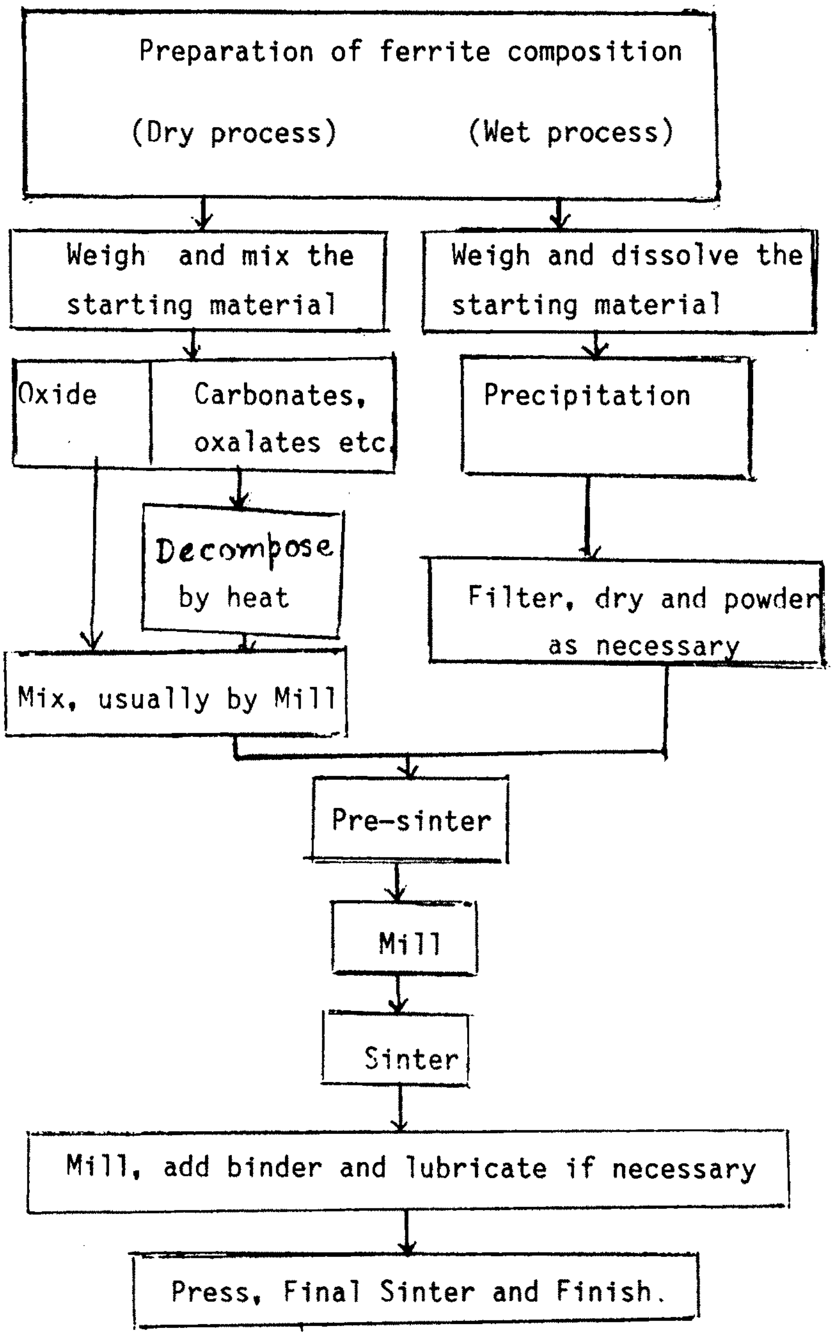

2.7 PRESINTERING :

The platinum crucibles with samples were kept in furnace and furnace was heated at the rate of 80°C per hour, upto 700°C for 12 hours. The temperature of the furnance was controlled by dimmerstat and required partial pressure of oxygen in the furnace was maintained How? throughout the heating period. The furnace was allowed to cool at the rate of 80°C per hour upto room temperature. For measuring temperature of furnace calibrated chromel alumel thermocouple was used.

2.8 GRINDING :

The crucibles were taken out from furnace, the samples were transferred to agate morter and grinded to form a fine powder. The grinding was carried out for three hours for each sample in AR grade acetone.

2.9 SINTERING :

Samples were then transferred to crucibles which were washed with chromic acid and cleaned. Crucible with samples were then kept in the furnace and furnace was heated at the rate of 80°C per hour upto 900°C. Samples were heated about 40 hours at 900°C temperature and temperature was maintained constant. Atmosphere and temperature Details inside the furnace were controlled so as to form complete solid solution and the furnace was then cooled at the rate 80°C per hour.

2.10 PELLET FORMATION :

Sintered samples were ground in acetone base and were seived to obtain uniform particle size. By using die of 1.0 cm diameter and pressure of 9 tonnes per square inch, pellets were formed. The polyvinyl acetate was used as binder.

2.12 FINAL SINTERING :

The pellets were kept on thin platinum foils and foils were then kept in furnace. The furnace was heated at the rate of 80°C per hour upto 900°C in about 12 hours. The pellets were kept at constant temperature of 900°C for 12 hours and due care was taken to control the furnace temperature. The furnace was then cooled at the rate of 80°C per hour.

B - X-RAY DIFFRACTION STUDY

X-ray diffraction technique is used to confirm the formation of ferrite samples and to characterise the crystal structure. In this section details of diffractometer are furnished. The peaks of dffractograms are indexed, the lattice constants, 'a' and 'd' values are calculated. The results on the crystallographic data are discussed.

2.13 THE DIFFRACTOMETER :

In the present work, Siemen's computerised diffractometer at Tata Institute of Fundamental Research, Bombay, was used. The particulars are as follows :

1) Target used : Cu
2) Wavelength λ : 1.54060 A°
3) Rate of scanning : 2° per minute
4) Range of 2θ : 15° to 65°
5) Operating voltage: 40 kV
6) Operating current: 40 mA

Along with diffractographs, the diffractometer provides the following information :

1) Angular position of the peak : 2θ
2) Corresponding "d" value as given by Bragg's realtion
3) Height of peaks
4) Percentage height of peaks.

2.14 PREPARATION OF THE SPECIMEN :

The specimen required for obtaining diffractographs was prepared in the following way. A very fine powder of the sample was pressed in the circular pit of diameter 1 cm of the holder and the surface was made perfectly plane by pressing the powder with glass slide which when used in skillful fashion, results in a plane surface of specimen. This was then placed in sample holder. The samples were scanned between 15° to 65° and the first reflection was observed at about $2\theta = 18°$.

2.15 INDEXING THE PEAKS IN DIFFRACTION PATTERN :

For a cubic lattice, the interplanar distance d_{hkl} are related by [9]

$$d_{hkl} = \frac{a}{(h^2+k^2+l^2)^{\frac{1}{2}}} \qquad \ldots \qquad (2.1)$$

Bragg's law is

$$2d_{hkl} \operatorname{Sin}\theta_{hkl} = n\lambda$$

and for $n = 1$

$$2d_{hkl} \operatorname{Sin}\theta_{hkl} = \lambda \qquad \ldots \qquad (2.2)$$

The "d" values are given along with "2θ" by computerised diffractometer.

The peak of 100% intensity corresponds to the plane (311) so the lattice parameter "a" in this case is calculated by relation (2.1). For other peaks, h, k, l values were determined by usual procedure[8,10] and peaks were indexed.

2.16 CURIE TEMPERATURE :

The critical temperature for a ferromagnetic or ferrimagnetic material, at which magnetic transformation takes place is called Curie temperature. It is the temperature below which, there is spontaneous magnetisation in absence of an externally applied magnetic field and above which the material is paramagnetic. In disordered state above Curie temperature thermal energy overrides any interactions between local magnetic moment. Below Curie temperature these interactions are predominent and cause local moments to order or to align, in such a way that there is a net spontaneous magnetisation.

Many physical properties show change in behaviour at this temperature. There is a peak in specific heat and magnetic permeability at Curie temperature. There is a change in elastic properties and thermal expansivity. The Curie temperature can be altered by changes in composition, pressure and other thermodynamic parameters.

2.17 APPARATUS AND DETERMINATION OF CURIE TEMPERATURE :

We have evaluated Curie temperature of our samples by the technique which is described below in detail. Loria et. al.[11] have suggested the method of determination of Curie temperatures. We have modified this technique. The method by Loria et. al. suffers from

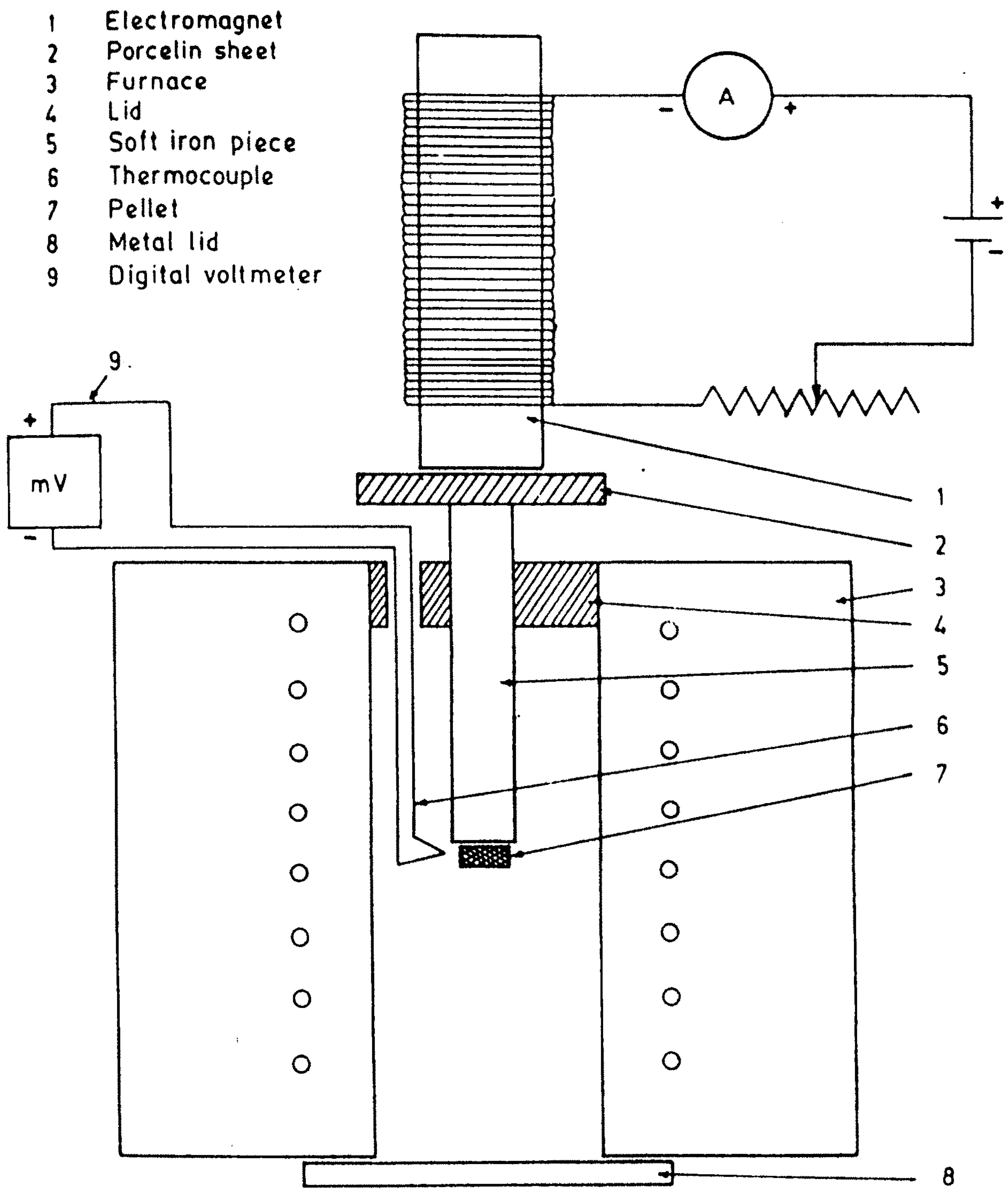

FIG. 2·14: SET UP FOR DETERMINATION OF CURIE TEMPERATURE(Tc).

a draw-back, that along with pellet the core of electromagnet is also subjected to heating, which causes a damage to the enamel of electromagnet wire, leading to short circuit. At the same time more current is required to obtain the substantial magnetisation. We have improved upon the technique, by not directly subjecting the core of the electromagnet to the temperature of furnace, instead of that induction technique is used for magnetising the specimen bar to which pellet is attached. Accurate measurement of Curie temperature is made by using chromel alumel thermocouple along with digital multimeter of least count 0.1 mV enabling measurement of temperature correctly. Fig. 2.14 shows this technique.

2.18 RESULTS AND DISCUSSION :

The allowed reflections in X-ray diffraction pattern for spinel structure[12] are as follows :

Cubic structure : (111), (220), (311), (222), (400), (422),
(333/511), (440).

Tetragonal : (111), (202), (220), (113), (311), (222),
(004), (400), (422), (511/333), (404), (440).

The xerox copies of indexed diffractograms are given in figures [2.1.1 to 2.1.10]. From the diffractograms it can be seen that all samples show well defined diffraction peaks. This suggests single phase formation, with no additional reflections. The diffracto grams indicate the formation of ferrite in our samples and confirm the spinel structure[8]. Crystallographic data for all samples is given in Table No. [$2.2A_1, A_6$ and B_1–B_6]. From the tables [2.2A to $2.2A_6$ and B_1 to B_6], it is seen that the calculated "d" values are in good agreement with observed "d" values. It was found that all samples exhibit cubic structure. The values of lattice parameter "a" for doped systems are reported in Tables 2.2. The calculated values of lattice parameter "a" show variation in the range which is being in the range of FCC spinel.

From Tables 2.2 it can be seen that the lattice parameter "a" remains almost unaffected by the doping of 0.02% and 0.05% mole wt. of Nb Fig. 2.1 and Fig. 2.2 show compositional variation of lattice parameter "a" in A° with content of Zn for mixed $Cu_xZn_{1-x}Fe_2O_4$ system when doped with 0.02 and 0.05 mole wt. percent of Nb. It is seen that lattice parameter increases almost linearly with addition of Zn^{+2} for values of x greater than 0.2 for both doped and mixed ferrites.[13] The systems obey Vegard's law. However, lattice parameter shows sharp rise for $x = 0$ to $x = 0.2$ in both doped and mixed systems. Lattice parameter is minimum for $CuFe_2O_4$, [doped with 0.02 and 0.05 mole wt. percent Nb] and maximum for $ZnFe_2O_4$ in doped and undoped systems.

The values of "a" for doped and mixed ferrite system are in close agreement with those reported earlier.[14,15,16]

The sudden rise in lattice parameter from $x = 0$ to $x = 0.2$ can be explained on the basis of ionic radii. . The ionic radii of Cu^{2+}, Zn^{2+}, Fe^{3+} are given in Table 2.3.

Tabel - 2.3

Ion	Ionic radius
Cu^{2+}	0.70 A°
Zn^{2+}	0.83 A°
Fe^{2+}	0.67 A°
Nb^{5+}	0.70 A°

As Zinc content increases, it will occupy A-site and displace Fe^{3+} ions to B site and number of Cu^{2+} ions on B site are reduced thereby increasing the lattice parameter.

Lattice parameter variation and magnetisation studies on Ti^{4+}, Zr^{4+}, Sn^{4+} and Nb^{5+} substituted Ni-Zn ferrites has been carried out by A.R.Das et al.[17]. On the basis of existing predictions[18,19,20], the proposed sites for Ti, Sn and Nb are B and for Zn^{2+} is A. The fact that addition of Nb^{5+} does not affect 'a' value suggests that its effect is masked by Zn^{2+} ions which have largest ionic volume.

In Table 2.4A and 2.4B data on X-ray density, number of molecules per unit cell and radii of A and B sites are reported. X-ray densities were calculated using the relation

$$D_x = \frac{8\ M}{Na^3}$$

M = Molecular weight

N = Avagrdro's number

a = Lattice parameter

Table 2.4 [A and B]

X-ray density, Radii of sites and molecules per unit cell

Sample	Material	X-ray density gm/cc	n	r_A(A°)	r_B(A°)
A_1	$ZnFe_2O_4$	5.2772	8	0.4983	0.7812
A_2	$Cu_{0.2}Zn_{0.8}Fe_2O_4$	5.3098	8	0.4986	0.7815
A_3	$Cu_{0.4}Zn_{0.6}Fe_2O_4$	5.3333	8	0.4947	0.7769
A_4	$Cu_{0.6}Zn_{0.4}Fe_2O_4$	5.3376	8	0.4932	0.7753
A_5	$Cu_{0.8}Zn_{0.2}Fe_2O_4$	5.3517	8	0.4907	0.7724
A_6	$CuFe_2O_4$	5.1215	8	0.4734	0.7524
B_1	$ZnFe_2O_4$	5.2276	8	0.4983	0.7812
B_2	$Cu_{0.2}Zn_{0.8}Fe_2O_4$	5.3078	8	0.4985	0.7814
B_3	$Cu_{0.4}Zn_{0.6}Fe_2O_4$	5.3447	8	0.4933	0.7754
B_4	$Cu_{0.6}Zn_{0.4}Fe_2O_4$	5.3616	8	0.4905	0.7722
B_5	$Cu_{0.8}Zn_{0.2}Fe_2O_4$	5.3733	8	0.4883	0.7696
B_6	$CuFe_2O_4$	5.6036	8	0.4621	0.7393

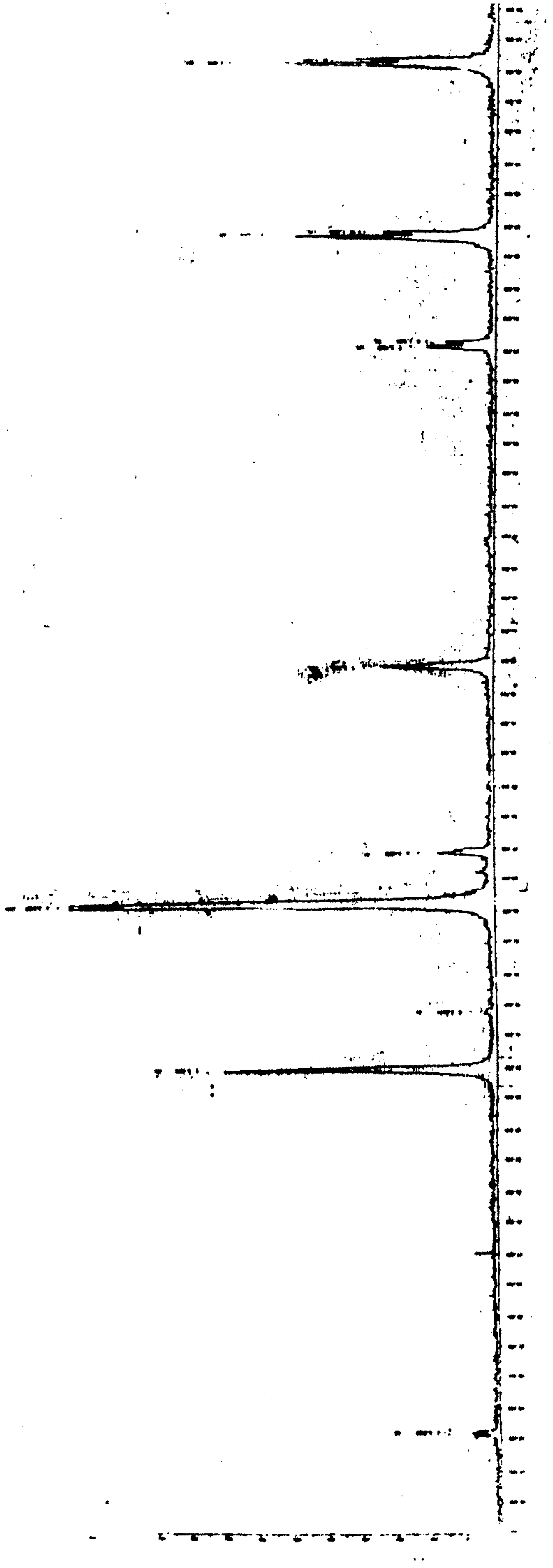

Fig. 2·1·1, A_1, $ZnFe_2O_4$

Fig 2·1·2, A_2, $Cu_{0.2}Zn_{0.8}Fe_2O_4$

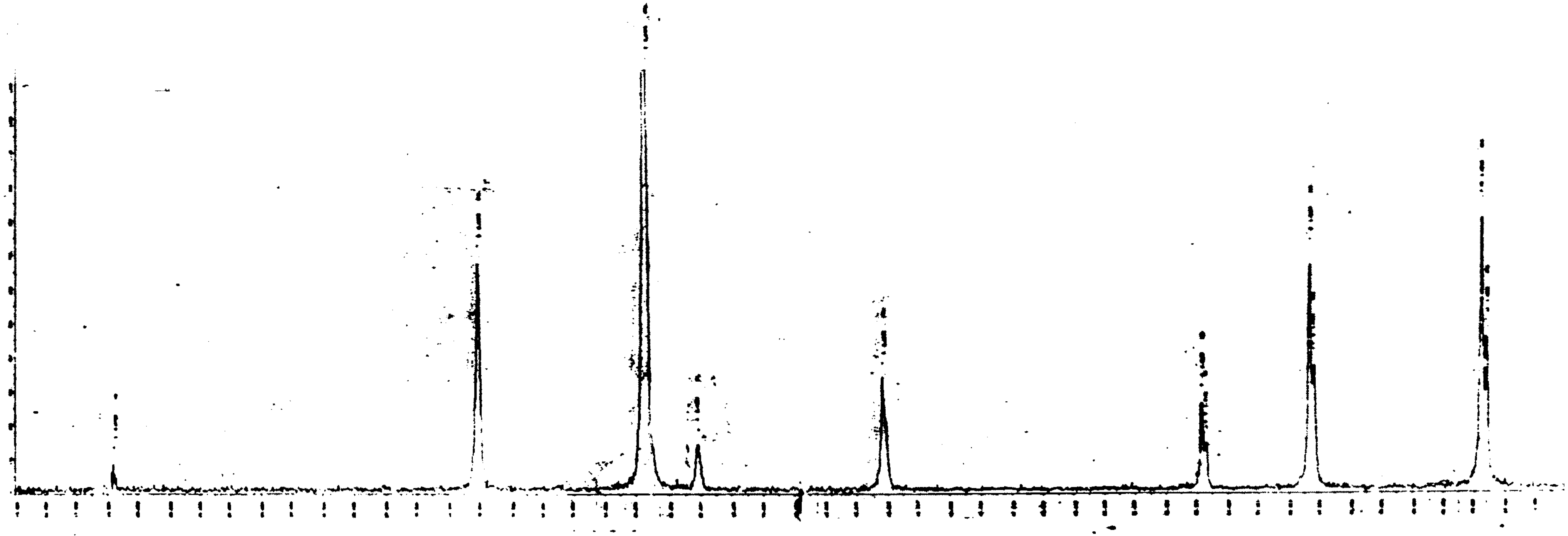

Fig 2.1.3 Az $Cu_{0.4}Zn_{0.6}Fe_2O_4$

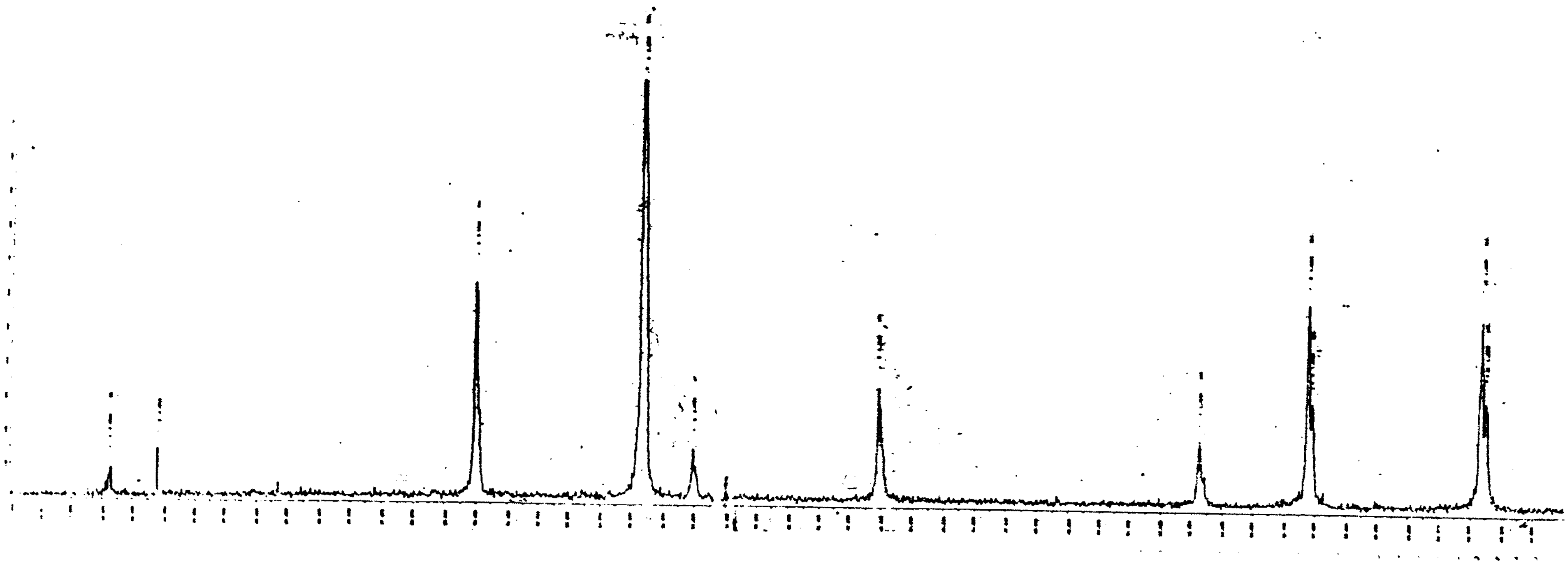

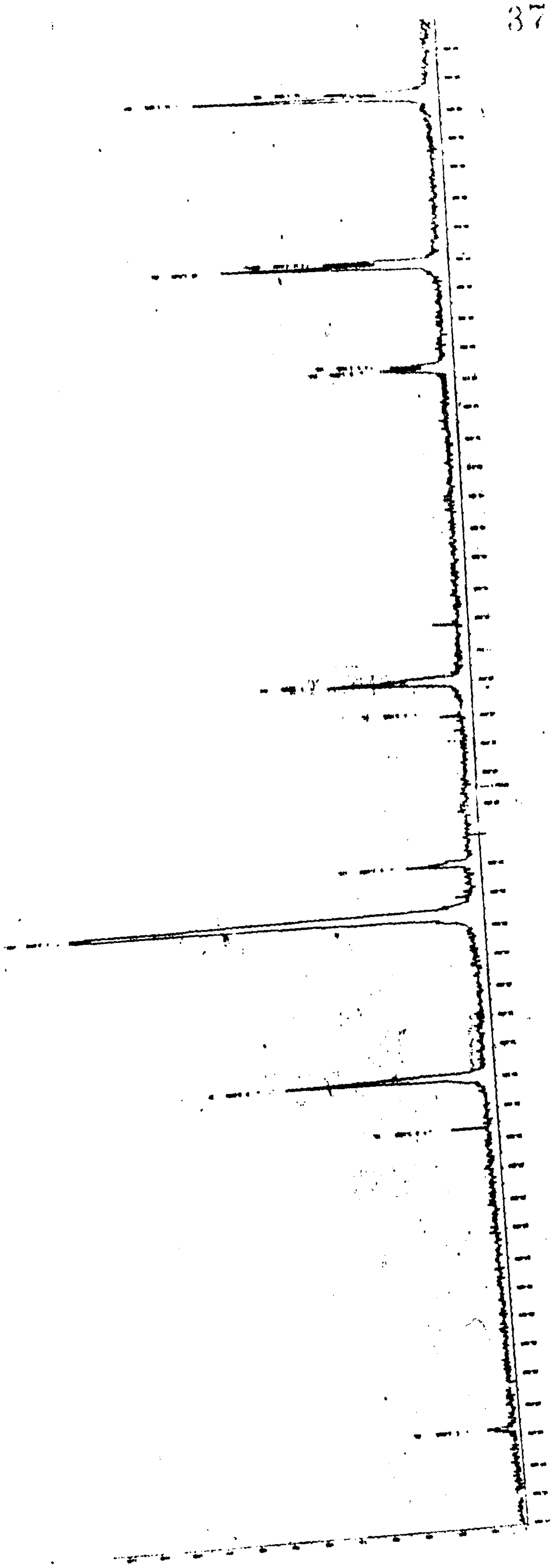

Fig 2.1.4, $Cu_{0.6}Zn_{0.4}Fe_2O_4$ (A4)

Fig 2.1.5, A5, $Cu_{0.8}Zn_{0.2}Fe_2O_4$

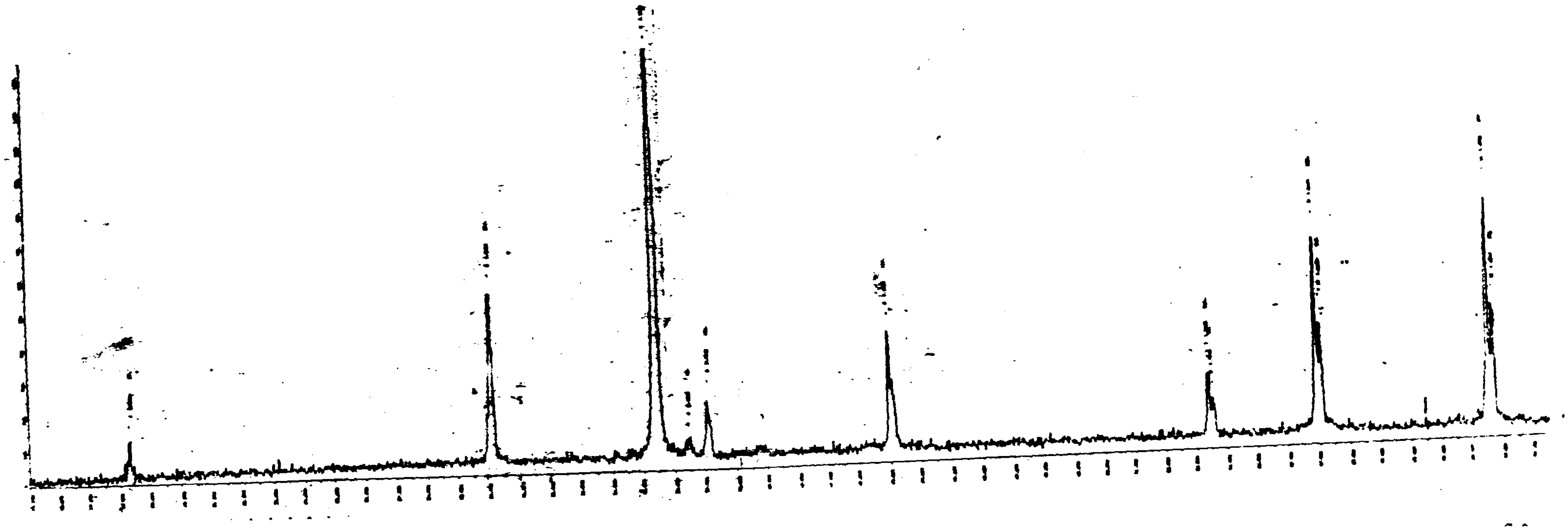

Fig 2·1·6, B_1; $ZnFe_2O_4$

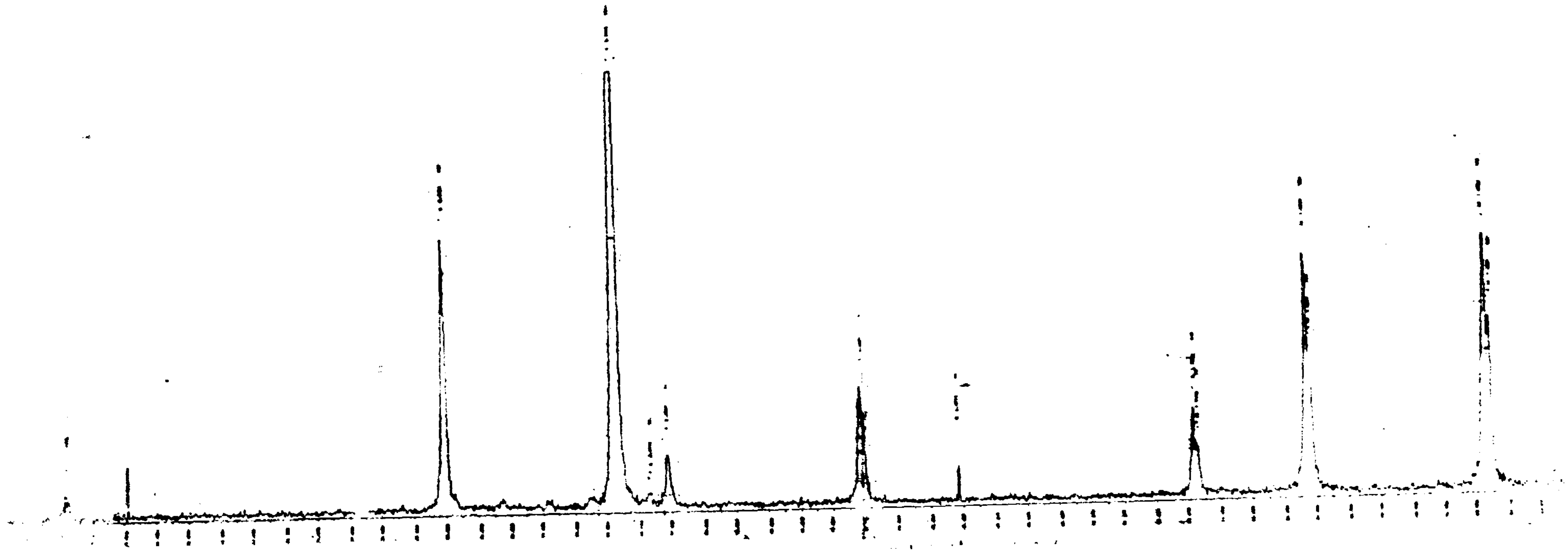

Fig 2.1.7, B_2; $Eu_{0.2}Zn_{0.8}Fe_2O_4$ (B_2)

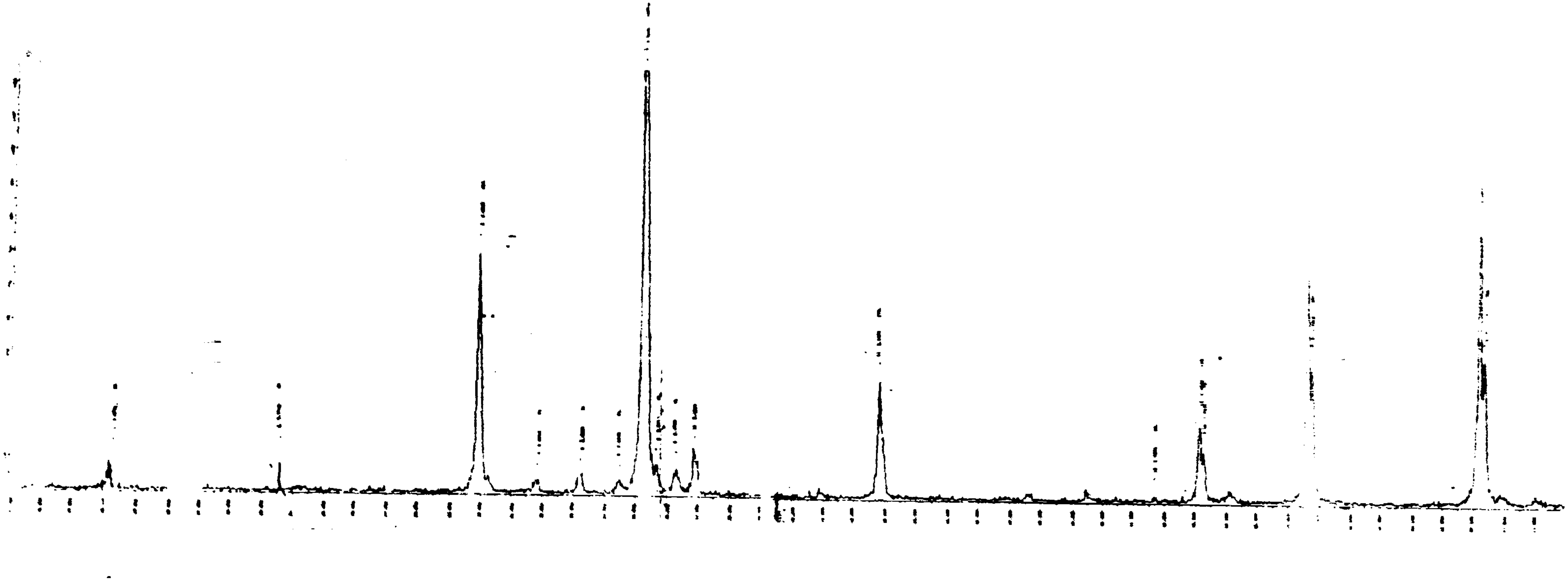

Fig 2.1.8, $Cu_{0.4}Zn_{0.6}Fe_2O_4$, (B_3).

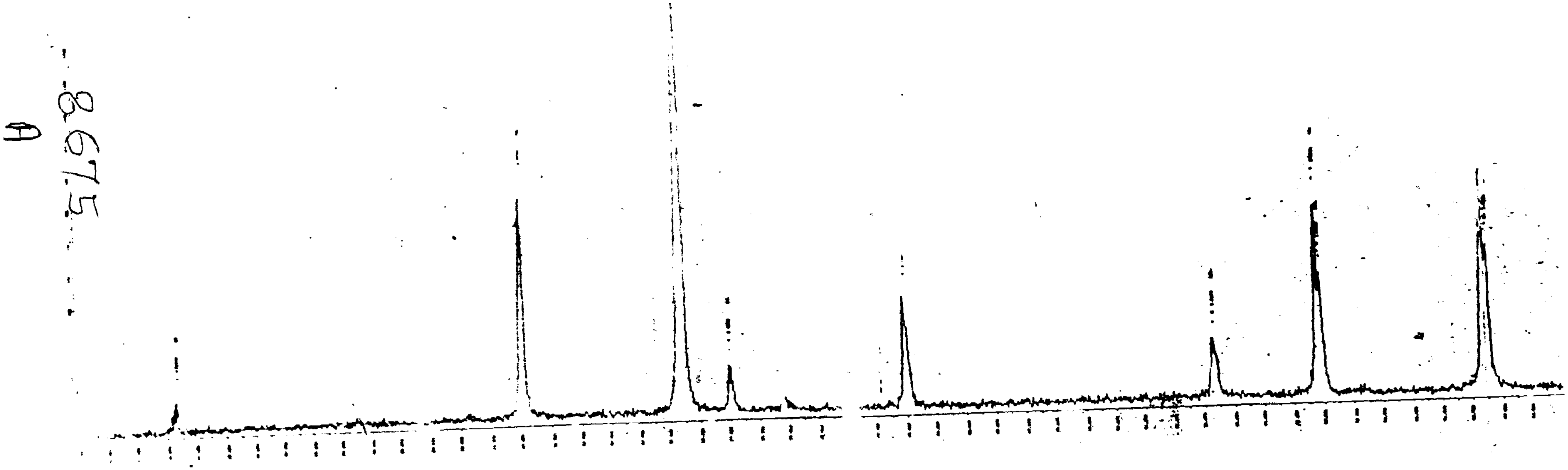

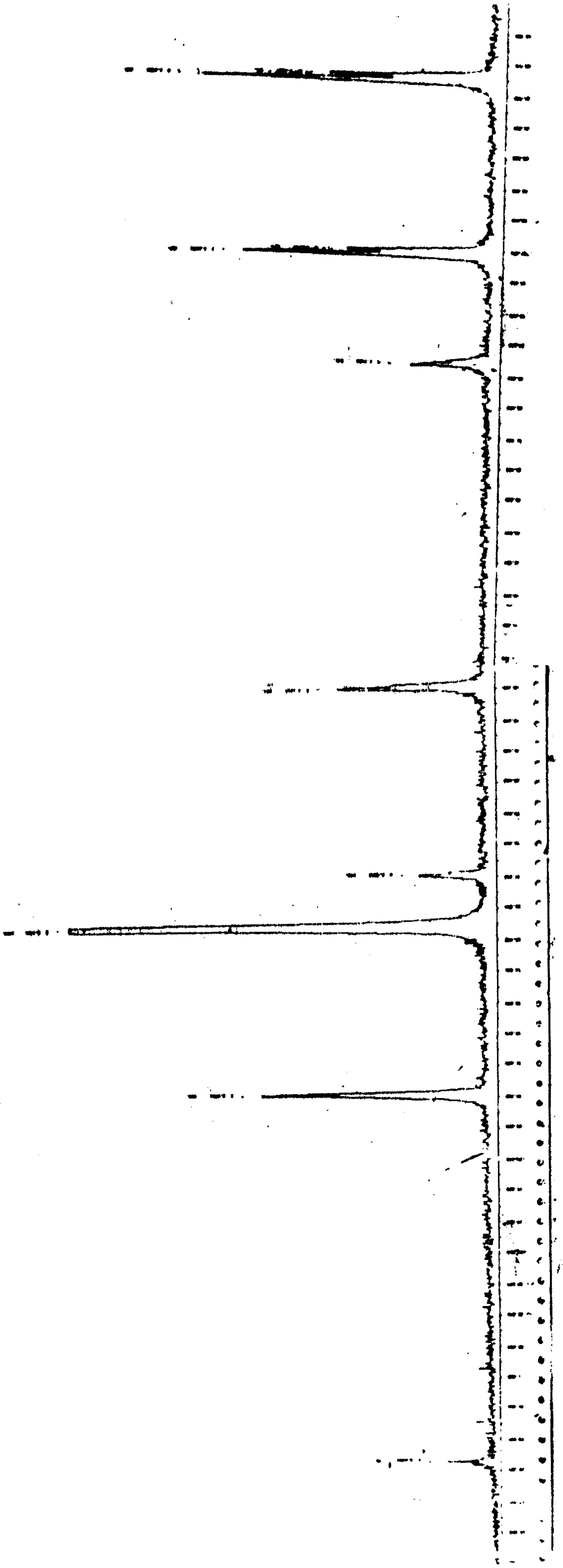

Fig 2.1.9 $Cu_{0.6}Zn_{0.4}Fe_2O_4$ (B4)

Fig 2.1.10, $Cu_{0.8}Zn_{0.2}Fe_2O_4$ (B5)

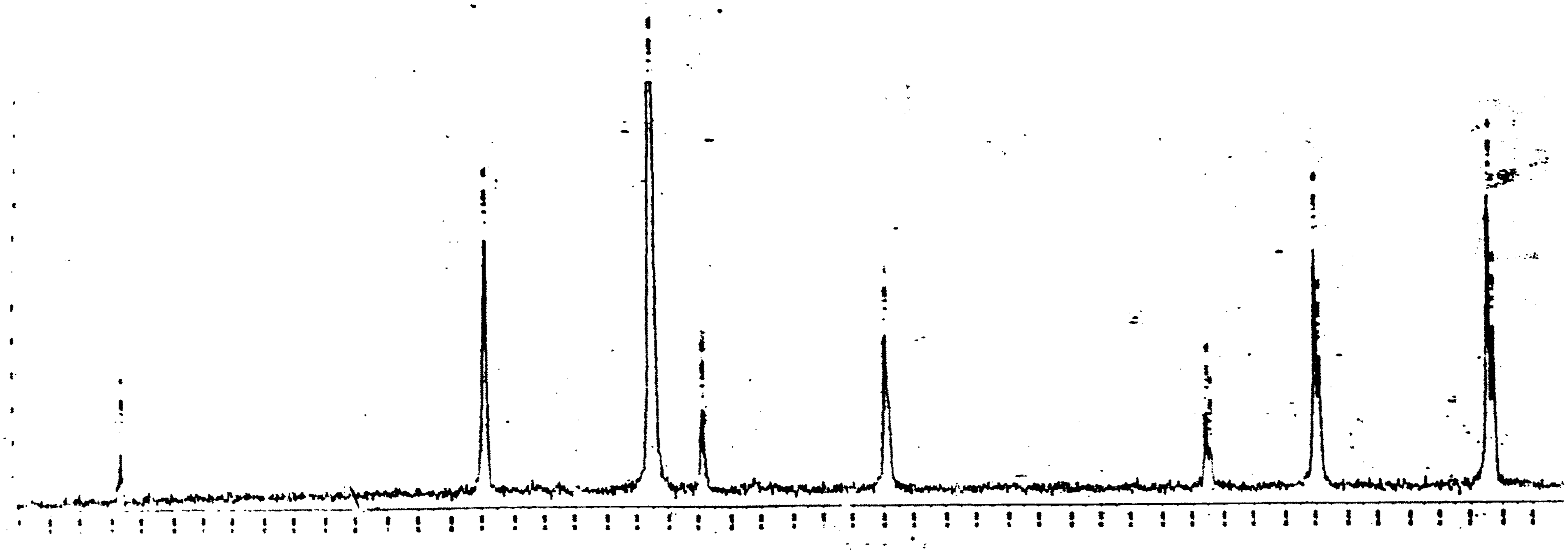

Table 2.2.A_1

Sample A_1-$ZnFe_2O_4$ 0.02 mole wt.% a=8.444844 A°

Sr.No. of peak	θ^0 deg	$d_{(obs)}$ A°	$d_{(cal)}$ A°	Plane hkl
1	9.095	4.8729	4.8756	111
2	14.962	2.9835	2.9857	220
3	15.890	2.8134	2.8857	310
4	17.626	2.5439	2.5439	311
5	21.411	2.1101	2.1112	400
6	26.62	1.7237	1.7237	422
7	28.297	1.6249	1.6252	511/333
8	31.15	1.4891	1.4928	440

Table 2.2.A_2

Sample A_2 : $Cu_{0.2}Zn_{0.8}Fe_2O_4$ 0.02 mole wt.% Nb^{+5} A=8.4462351

Sr.No. of peak	θ^0 deg	$d_{(obs)}$ A°	$d_{(cal)}$ A°	Plane hkl
1	9.007	4.8720	4.8764	111
2	17.627	2.5438	2.5463	311
3	18.44	2.4353	2.4382	222
4	21.423	2.1090	2.1115	400
5	26.561	1.7227	1.7240	422
6	28.319	1.6238	1.6254	511/333
7	31.1	1.4913	1.4930	440
8				

Table 2.2.A_3

Sample A_3 : $Cu_{0.4}Zn_{0.6}Fe_2O_4$ 0.02 mole Wt.% Nb^{5+} A=8.4279

Sr.No. of peak	θ° deg	$d_{(obs)}$ A°	$d_{(cal)}$ A°	Plane hkl
1	9.121	4.8594	4.8658	111
2	14.997	2.9768	2.9797	220
3	17.662	2.5388	2.5411	311
4	18.472	2.4305	2.4329	222
5	21.467	2.1048	2.1069	400
6	26.617	1.7193	1.7203	422
7	28.54	1.6169	1.6219	511/333
8	31.154	1.4890	1.4898	440

Table 2.2.A_4

Sample A_4 : $Cu_{0.6}Zn_{0.4}Fe_2O_4$ 0.02 mole Wt.% Nb^{5+} a=8.4212

Sr.No. of peak	θ° deg	$d_{(obs)}$ A°	$d_{(cal)}$ A°	Plane hkl
1	9.12	4.8615	4.8620	111
2	15.008	2.9746	2.9773	220
3	17.677	2.5368	2.5391	311
4	18.489	2.4290	2.4310	222
5	21.485	2.1031	2.1053	400
6	26.649	1.7174	1.7189	422
7	28.398	1.6197	1.6206	511/333
8	31.186	1.4876	1.4886	440

Table 2.2.A_5

Sample A_5 : $Cu_{0.8}Zn_{0.2}Fe_2O_4$ 0.02 mole Wt.% Nb^{5+} a=8.409738 A°

Sr.No. of peak	θ° deg	$d_{(obs)}$ A°	$d_{(cal)}$ A°	Plane hkl
1	9.144	4.8469	4.8553	111
2	15.034	2.9695	2.9732	220
3	17.702	2.5333	2.5336	311
4	18.525	2.4245	2.4276	222
5	21.508	2.1010	2.1024	400
6	26.69	1.7150	1.7166	422
7	28.442	1.6174	1.6184	511/333
8	31.239	1.4853	1.4866	440

Table 2.2.A_6

Sample A_6 : $CuFe_2O_4$ 0.02 mole Wt.% Nb^{5+} A=8.3272195A°

Sr.No. of peaks	θ° deg	$d_{(obs)}$ A°	$d_{(cal)}$ A°	Plane hkl
1	9.144	4.8553	4.8469	111
2	14.974	2.9812	2.9441	220
3	17.885	2.5082	2.5107	311
4	18.554	2.4207	2.5038	222
5	21.825	2.0736	2.0818	400
6	23.123	1.9615	1.9627	411/330
7	26.911	1.7019	1.6997	422
8	28.822	1.5978	1.6025	511/333
9	31.699	1.4660	1.4720	440

Table 2.2.B$_1$

Sample B$_1$: ZnFe$_2$O$_4$ 0.5 mole Wt.% Nb^{5+} a=8.4450742 A°

Sr.No. of Peak	θ deg	$d_{(obs)}$ A°	$d_{(cal)}$ A°	Plane hkl
1	9.099	4.8711	4.8757	111
2	11.783	3.7722	3.7767	210
3	14.965	2.9829	2.9857	220
4	15.914	2.8093	2.8150	300/221
5	17.625	2.5440	2.5462	311
6	18.434	2.4360	2.4378	222
7	21.416	2.1096	2.1112	400
8	26.558	1.7229	1.7238	422
9	28.301	1.6248	1.6414	511/333
10	31.073	1.4924	1.4928	440

Table 2.2.B$_2$

Sample B$_2$: Cu$_{0.2}$Zn$_{0.8}$Fe$_2$O$_4$ 0.05 mole Wt.% Nb, a=8.4457697 A°

Sr.No. of Peak	θ deg	$d_{(obs)}$ A°	$d_{(cal)}$ A°	Plane hkl
1	9.09	4.8721	4.8761	111
2	14.965	2.9830	2.9860	220
3	17.624	2.5422	2.5464	311
4	18.436	2.4357	2.4380	222
5	21.420	2.1088	2.1144	400
6	26.563	1.7226	1.7239	422
7	28.39	1.6201	1.6253	511/333
8	31.098	1.4914	1.4930	440

Table 2.2.B_3

Sample B_3 : $Cu_{0.4}Zn_{0.6}Fe_2O_4$ 0.05 mole Wt.% Nb, a=8.421944A°

Sr.No. of Peak	θ deg	$d_{(obs)}$ A°	$d_{(cal)}$ A°	Plane hkl
1	9.142	4.8483	4.8624	111
2	15.015	2.9732	2.9776	220
3	17.675	2.5370	2.5393	311
4	18.486	2.4293	2.4312	222
5	21.475	2.1041	2.1054	400
6	26.633	1.7184	1.7191	422
7	28.371	1.6210	1.6208	511/333
8	31.22	1.4861	1.4860	440

Table 2.2.B_4

Sample B_4 : $Cu_{0.6}Zn_{0.4}Fe_2O_4$ 0.05 mole Wt.% Nb a=8.4088195A°

Sr.No. of Peak	θ deg	$d_{(obs)}$ A°	$d_{(cal)}$ A°	Plane hkl
1	9.142	4.8484	4.8548	111
2	15.031	2.9701	2.9729	220
3	17.704	2.5331	2.5353	311
4	18.519	2.4252	2.4274	222
5	21.5075	2.1010	2.1022	400
6	26.674	1.7159	1.7164	422
7	28.4305	1.6180	1.6127	511/333
8	31.219	1.4861	1.4864	440

Table 2.2.B_5

Sample B_5 : $Cu_{0.8}Zn_{0.2}Fe_2O_4$ 0.05 mole Wt.% Nb a=8.3984 A°

Sr.No. of Peak	θ deg	$d_{(obs)}$ A°	$d_{(cal)}$ A°	Plane hkl
1	9.147	4.8452	4.8488	111
2	15.053	2.9660	2.9693	220
3	17.726	2.5300	2.5341	311
4	18.543	2.4222	2.4244	222
5	21.840	2.0980	2.0997	400
6	26.716	1.7134	1.7144	422
7	28.476	1.6156	1.6127	511/333
8	31.275	1.4838	1.4847	440

Table 2.2.B_6

Sample B_6 : $CuFe_2O_4$ 0.05 mole Wt.% Nb a=8.2774 A°

Sr.No. of Peak	θ deg	$d_{(obs)}$ A°	$d_{(cal)}$ A°	Plane hkl
1	9.188	4.8343	4.7789	111
2	15.35	2.9099	2.9265	220
3	17.293	2.5913	2.6175	310
4	17.994	2.4935	2.4956	311
5	18.583	2.4171	2.3894	222
6	21.993	2.0569	2.0693	400
7	29.019	1.5879	1.5929	511/333
8				

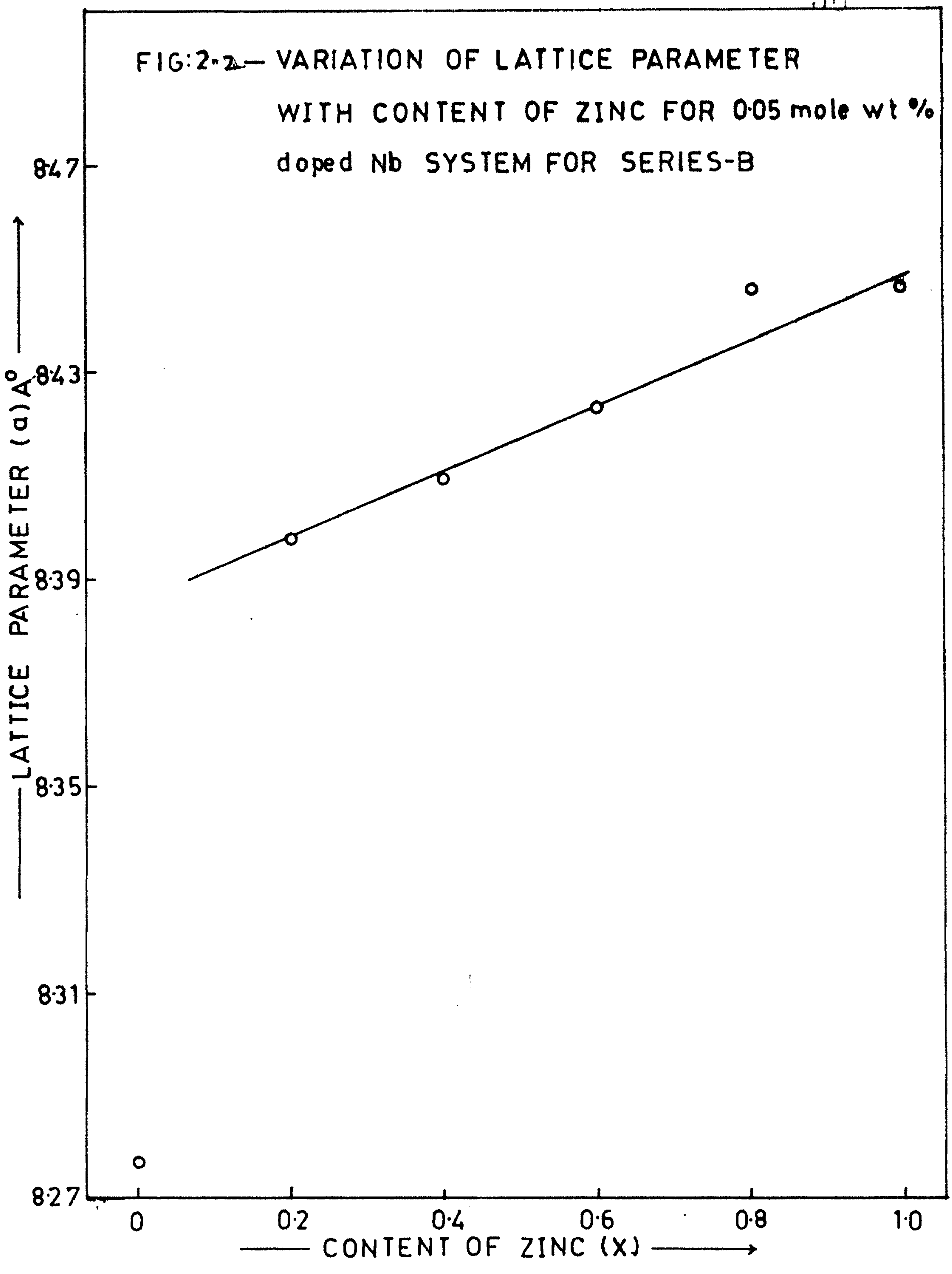

FIG:2·2— VARIATION OF LATTICE PARAMETER WITH CONTENT OF ZINC FOR 0·05 mole wt % doped Nb SYSTEM FOR SERIES-B

FIG:2·[illegible] —VARIATION OF LATTICE PARAMETER WITH CONTENT OF ZINC FOR 0·02 mole wt % doped Nb SYSTEM FOR SERIES-A

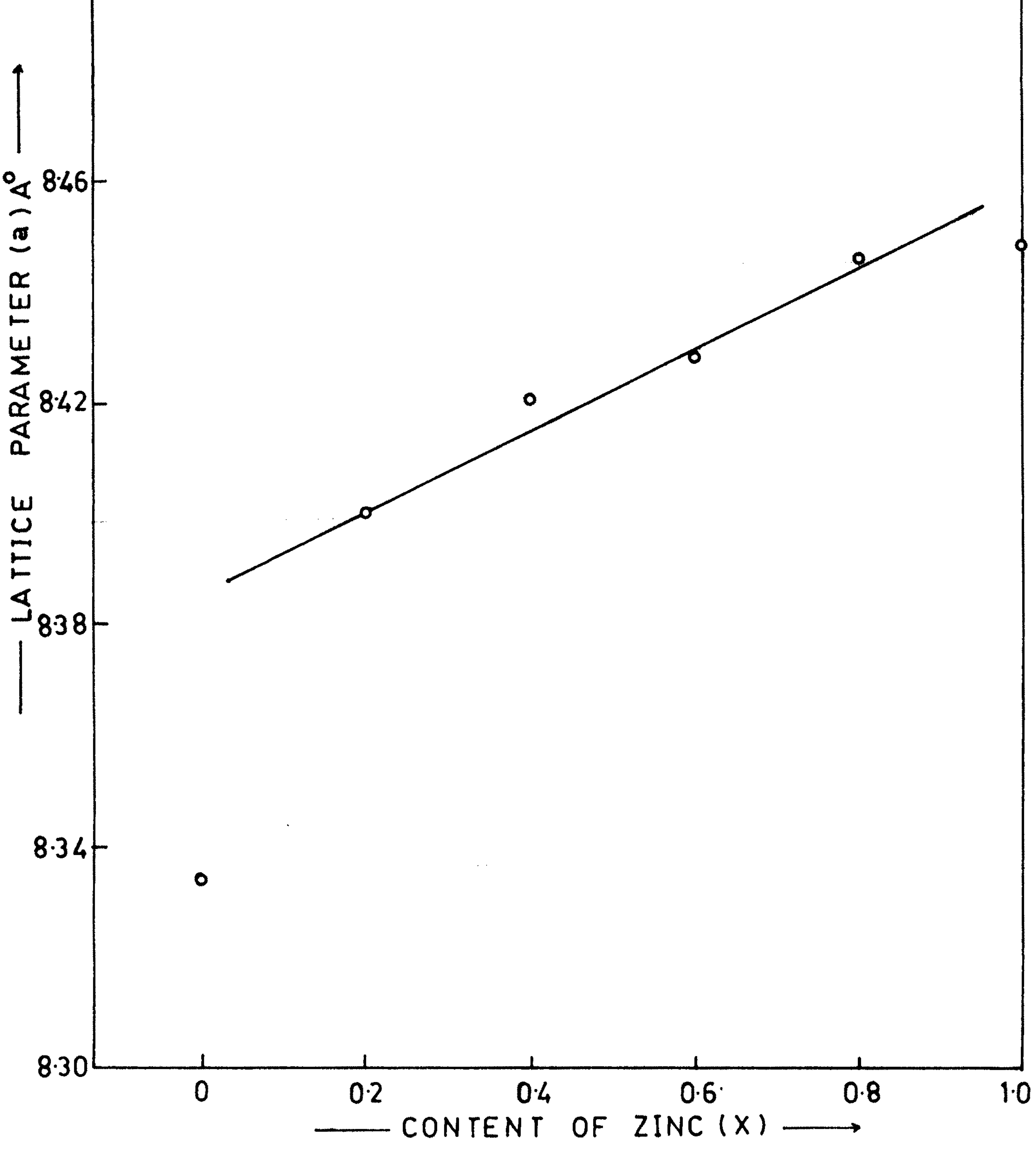

The number of molecules for unit cell were evaluated[21]

$$n = \frac{N\rho a^3}{M} \qquad \ldots \qquad (2.3)$$

where

ρ = X-ray density gm/cc

M = Molecular weight

N = Avogadro 's Number

a = Lattice constant

Radii of "A" and "B" sites were calculated using formulae given below

$$r_A = (u - \tfrac{1}{4})\ a\ (3)^{\frac{1}{2}} - r(O^{-2}) \qquad \ldots \qquad (2.4)$$

$$r_B = (5/8 - U)\ a - r(O^{-2}) \qquad \ldots \qquad (2.5)$$

U = 3/8 = oxygen ion parameter (in ideal case),

$r^{0-2} = 1.33$ A°

The variation of r_A and r_B with addition of Zn is as shown inTable 2.4 It is seen that both 'r_A' and 'r_B' values increase in an almost linear fashion with addtion of Zn^{2+}. Similar behaviour is observed for doped systems. The number of occupying lattice position per unit cell has been obtained and is equal to eight in all cases, confirming FCC Bravis lattice crystal structure of the doped mixed ferrite samples.

Bond lengths R_A and R_B have been calculated using formulae

$$R_A = a/3\ (\delta + 1/8) \qquad \ldots \qquad (2.6)$$

$$R_B = (3\delta^2 - \delta/2 + 1/16)^{\frac{1}{4}} \qquad \ldots \qquad (2.7)$$

δ = u- 375 deviation from u value.

These calculated values of bond lengths are reported in Table (2.5).

Table (2.5A and 2.5B) show variation of R_A and R_B with content of Zn^{2+} for doped mixed ferrite system. It is seen that R_A and R_B increase with increase of Zn content.

The increase in average bond length R_A can be correlated with increase in value of lattice parameter "a" with the content of Zn .[22] As Zn content in both the doped mixed system increases, the presence of Zn^{2+} ions on A-site increases. Since $ZnFe_2O_4$ is normal spinel Zn^{2+} ions occupy "A" sites only. The bond length R_A increases with increase in content of Zn^{2+} in both doped systems. Increase in value of R_B with increase in Zn^{2+} content can be explained on the similar lines. Levine's[23] recent work on bond susceptibilities in spinels shows that decrease in bond length corresponds to increase in covalent character.[24] From Table 2.4 and 2.5 it is seen that for both doped and mixed ferrite system A-O as well B-O distances go on increasing with decrease in copper content. Hence doped ferrite $Cu_{0.8}Zn_{0.2}Fe_2O_4$ is more covalent than undoped $Cu_{0.2}Zn_{0.8}Fe_2O_4$ or it can be concluded that the covalency decreases from $CuFe_2O_4$ to $ZnFe_2O_4$ for both doped and mixed systems.

The values of X-ray densities and percentage porosities for mixed ferrite system doped with 0.02 % and 0.05 % weight percent Nb were calculated using formulae

$$D_x = \frac{8\ M}{Na^3} \qquad \ldots \qquad (2.8)$$

M = Molecular weight
N = Avogadro's number

a = Lattice constant

D_x = X-ray density

$$P = \text{Porosity} = -\frac{D_x - D_A}{D_x} \times 100\ \% \qquad \ldots \qquad (2.9)$$

D_A = Physical density.

The variation of X-ray density with increase of Zn content shows linear relation in all three cases. However, density of doped mixed ferrite systems go on increasing for the same content of Zn as compared to undoped system.

From the Table (2.6) it is seen that the values of percentage porosity (p) for both doped mixed ferrite system go on increasing with increase in Zn content.

Studies on doping of V_2O_5 in NiZn ferrite by Ram Narayan et. al.[26] and doping of 0.01% wt. ZrO_2 in ZnMg ferrites by Kolekar et. al.[27] have reported densification effect.

Table 2.5 [A and B]

Bond lengths R_A and R_B

Sample	Material	R_A A°	R_B A°
A_1	$ZnFe_2O_4$	1.8283	2.1121
A_2	$Cu_{0.2}Zn_{0.8}Fe_2O_4$	1.8286	2.1155
A_3	$Cu_{0.4}Zn_{0.6}Fe_2O_4$	1.8247	2.1069
A_4	$Cu_{0.6}Zn_{0.4}Fe_2O_4$	1.8232	2.1053
A_5	$Cu_{0.8}Zn_{0.2}Fe_2O_4$	1.8207	2.1024
A_6	$CuFe_2O_4$	1.8034	2.0824
B_1	$ZnFe_2O_4$	1.8283	2.1112
B_2	$Cu_{0.2}Zn_{0.8}Fe_2O_4$	1.8285	2.1114
B_3	$Cu_{0.4}Zn_{0.6}Fe_2O_4$	1.8233	2.1055
B_4	$Cu_{0.6}Zn_{0.4}Fe_2O_4$	1.8205	2.1022
B_5	$Cu_{0.8}Zn_{0.2}Fe_2O_4$	1.8183	2.0996
B_6	$CuFe_2O_4$	1.7921	2.0693

Table 2.6

Percentage Porosity

Material	A series 0.02 Mole wt.% Nb	B series 0.05 Mole wt.% Nb
$ZnFe_2O_4$	30.7670	22.6197
$Cu_{0.2}Zn_{0.8}Fe_2O_4$	30.6665	21.0698
$Cu_{0.4}Zn_{0.6}Fe_2O_4$	30.6720	20.0525
$Cu_{0.6}Zn_{0.4}Fe_2O_4$	28.9562	18.8654
$Cu_{0.8}Zn_{0.2}Fe_2O_4$	26.8589	16.9548
$CuFe_2O_4$	23.2746	12.1207

FIG:2A5 — VARIATION OF POROSITY WITH CONTENT OF ZINC FOR DOPED Cu-Zn SYSTEM

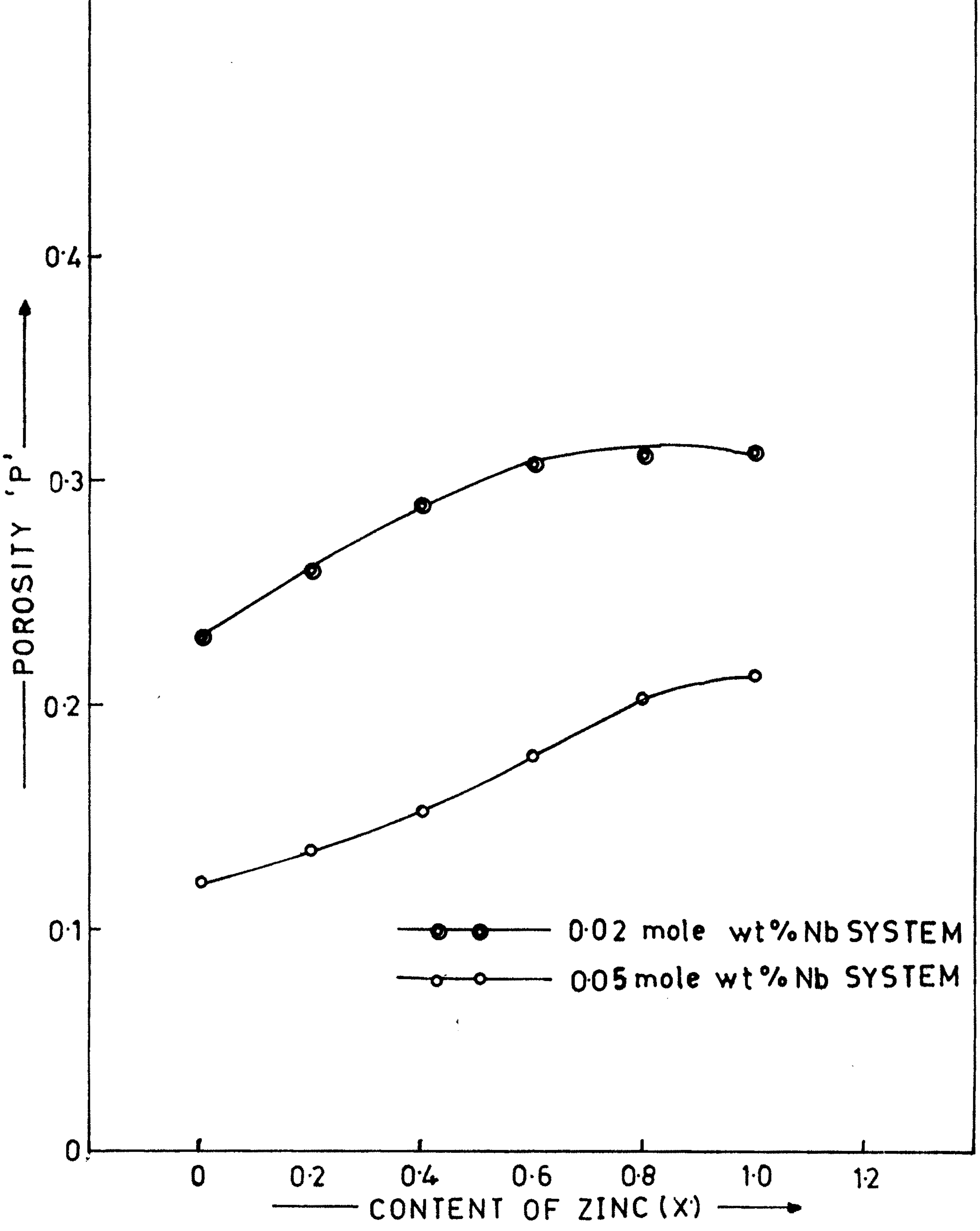

Table 2.7

A - 0.02 mole wt.% Nb^{5+} B - 0.05 mole wt.% Nb^{5+} doped

Composition	T_c(°K) By Exprimental		T_c(°K) By Graph	
	A	B	A	B
$ZnFe_2O_4$	-	-	-	-
$Cu_{0.2}Zn_{0.8}Fe_2O_4$	-	-	-	-
$Cu_{0.4}Zn_{0.6}Fe_2O_4$	512.5	490	510	498
$Cu_{0.6}Zn_{0.4}Fe_2O_4$	560	542	548	535
$Cu_{0.8}Zn_{0.2}Fe_2O_4$	564	579	571.5	560
$CuFe_2O_4$	615	635	623	620

REFERENCES :

1. Toshio Takada, M.Kiyama "Ferrite" Proc. Int. Conf. Tokyo, Japan p. 61 (July 1970).
2. Donald G., Wickhman, "Ferrite" Proc. Int. Conf. Tokyo Japan p. 105 (July 1970).
3. Toshihiko Sata, Chinji Kuroda, Minorce Sato "Ferrite" Proc. Int. Conf. Tokyo Japan p.72 (July 1970).
4. Gorter,E., Proc. IRE 42(2) 1945 (1955).
5. Bozorth R.M., "Ferrimagnetism" p. 244 (1951) van Nortrand, Netherland.
6. Vent J.J. and Gorter E.W., Philips, Tech.Rev. 13, 181 (1952).
7. Wagner C.Z. Phys. Chem. B-34, 309-316 (1936).
8. Standley K.J. "Oxide Magnetic Material", Clearondon Press, New York, Chap. 2 p.9 (1972).
9. Henery N.F.M. Lipsen H. and Wooster W.A. "The Interpretation of X-ray diffraction photographic" MacMillan and Co.Ltd., London (1961).
10. Cullity B.D. "Elements of X-ray diffraction" Addison Wesley Publishing Co. Inc. England (1959).
11. K.K.Loria and Sinha,A.P.B., Ind. J. Pure.Appl.Phys. Rev. B 19, 499 (1979).
12. Bergstein,A. and Cevinka,L."Influence of Mn and oxygen content on tetragonal deformation of copper ferrite." Czech J.Phys. B 11, p. 584 (1961).
13. Verway,E.J.W. and Heilmann, E.L.J.Chem. and Physi. 15, 174 (1947).

14. Delorme C. Bull. Soc. Franc. Min Crist. 81 (79) (1958).

15. Satyamurthy N.S., Natera M.G. and Youseef S.I., Phys. Rev. 181, 696 (1969).

16. Kulkarni R.G., Patil V.U. "Jr. Mat. Sci. GB, 17 843 (1982).

17. A.R.Das, Ananthan V.S. and Khan D.C., Indian Institute of Technology, Kanpur(208016) India.

18. Gorter,E.W., Phillips Res. Rep. 8, 403 (1954).

19. Puri,R.K. and Varshney Usha, J.Phys. Chem. Solids (44) 655 (1983).

20. Blasse,G., Phillips Resd. Rep. 18, 400 (1963).

21. Warren B.E. "X-ray diffraction" Addison Wesley Pub.Co. London Chap. V (1969).

22. Sawant,S.R. and Patil,R.N. J.Mat.Sci. 3496 (16) (1981).

23. Levine B.F., Physical Review, B 7, 2591 (1973).

24. Balal M.M., Mande C.I., J.Phys. & Chm. Sol. 38 843 (1977).

25. Yamashiro T., Jap. J. Appl. Phys. 12, 148 (1973).

26. Ram Narayan, Tripathi R.B., Das B.K. and Jain G.C., J.Mates. Sci. 18, 1267 (1983).

27. Kokekar,C.B. M.Phil. Thesis, Shivaji University, p.69.